JOURNAL OF MATERIALS SCIENCE **35** (2000) 4459 – 4463

Electrical properties of Li_2O-La_2O_3-SiO_2 electrode glasses after Ta_2O_5 doping and Ta implantation

P. W. WANG*
Department of Physics and Materials Research Institute, The University of Texas at El Paso, El Paso, TX 79968, USA

WANG CHENGYU, FU XIANPING, TAO YING
Institute of Glass and Inorganic New Materials, Dalian Institute of Light Industry, People's Republic of China
E-mail: pwang@utep.edu.

Electrical conductivities, σ, of the Li_2O-La_2O_3-SiO_2 glasses were investigated as functions of Ta_2O_5 doping and Ta ion-implantation. A linear relationship between logarithm σ and the inverse of the sample temperature, T, was found in 2 to 4 mol% Ta_2O_5 doped Li_2O-La_2O_3-SiO_2 glasses. The conductivity increases as Ta_2O_5 content increases at sample temperatures above 100°C. Fluences of 50 keV Ta ions per cm^2 from 5×10^{16} to 2×10^{17} were implanted into 0% and 2% Ta_2O_5 containing Li_2O-La_2O_3-SiO_2 glass samples. The activation energy of the conductivity was deduced from the relation between log σ and $1/T$. It was found in implanted samples that the conductivity increased, but the activation energy and $T_{k\text{-}100}$ decreased, where $T_{k\text{-}100}$ is the sample temperature when the conductivity reaches 100×10^{-1} S/cm. However, the Ta_2O_5 containing implanted samples show higher conductivities, lower activation energies and lower $T_{k\text{-}100}$. X-ray photoelectron spectroscopy (XPS) was used to study the structural modification introduced by implantation. Bridging oxygen (BO) and non-bridging oxygen (NBO), were observed in all samples. The changes in relative concentrations of BO and NBO before and after implantation clearly indicate the structure modification which results in the increase of the conductivity. It was clearly demonstrated in this study that both doping Ta_2O_5 and implanting Ta ions enhance the conductivity of Li_2O-La_2O_3-SiO_2 electrode glasses. *© 2000 Kluwer Academic Publishers*

1. Introduction

Since the electrical potential difference created between the surface of a thin glass electrode film and a solution is proportional to the pH value of the solution, the glass electrode is widely used to measure the pH value of aqueous solutions. It is expected that the electrode glass not only has high chemical stability to resist corrosion in the solution but also a low resistivity to increase the sensitivity of the pH meter.

Nikolskii *et al.* [1] found suitable compositions in Li_2O-La_2O_3-SiO_2 electrode glass after studying the properties of electrode glasses as functions of their compositions. Appen [2] summarized the electrical properties of silicate glasses doped with Ta_2O_5. Ross *et al.* [3] then doped 0% to 2% Ta_2O_5 into glasses and developed highly chemically stable electrode glasses.

In this paper, the electrical properties of Li_2O-La_2O_3-SiO_2 electrode glasses were investigated after doping Ta_2O_5 and implanting Ta ions into Li_2O-La_2O_3-SiO_2 electrode glasses. The conductivity changes caused by the implantation are deduced from the structural modification, which is determined by the relative concentrations of bridging oxygen (BO) and non-bridging oxygen (NBO) obtained from XPS measurements.

2. Experimental procedure

The compositions of the electrode glasses used in this work are listed in Table I. Samples were fabricated by using analytically pure chemicals, mixed and put in a platinum crucible, melted in a furnace at a temperature between 1300 and 1350 °C, formed into slabs and annealed at 525 °C, then cut into 12 × 12 × 2 mm pieces, then polished and cleaned by methanol and deionized water.

The ion implantation was done in a MEVVA IV 80-10 implanter. The implantation energy of Ta^+ ions was 50 keV and the fluences were $5\times$, $10\times$, and 20×10^{16} ions/cm^2. Singly charged Ta ions were selected by the mass spectrometer and implanted into the sample substrate in order not to significantly disturb the electron charge distribution of the sample. The volume conductivity of the sample from 20 to 400 °C

---

* Author to whom all correspondence should be addressed.

TABLE I The compositions of sample glasses (in mol%)

Sample No.	Li_2O	La_2O_3	Ta_2O_5	SiO_2
1	28	7	0	65
2	28	6	1	65
3	28	5	2	65
4	28	3	4	65
5	27	7	0	66
6	27	7	2	64
7	28	5.5	0	66.5
8	28	5.5	2	64.5

was determined by using ZL-5 model LCR meter in which a 12 to 10^5 Hz ac frequency was applied.

X-ray Photoelectron Spectroscopy (XPS) spectra were taken using a PHI 560 model Perkin Elmer surface analysis system. The base pressure of the ultra-high vacuum chamber during experiments was maintained at $1\text{–}3 \times 10^{-9}$ Torr. XPS spectra of the core level photoelectrons of O 1s were collected and investigated. Emission of photoelectrons was induced by Al K_α X-rays generated by 14 keV electrons impacting on aluminum at the 225 W power level. The pass energy of the double-pass cylindrical mirror energy analyzer was 50 eV which provides 1 eV resolution. The uncertainty is ±0.5% in relative concentration, and ±0.05 eV in binding energy (BE). Information from the XPS spectra can be obtained by use of a curve fitting program in which the peak position is the binding energy and the integrated area of the peak is related to the concentration of the element.

3. Results and discussion

3.1. Ta_2O_5 doping

The volume conductivities, σ, of samples 1–4 doped with various concentrations of Ta_2O_5 measured at different temperatures, T, are shown in Fig. 1. It is clearly seen that a linear relationship between log σ and $1/T$ is exhibited but the slope of the line changes at $T = 100\,^\circ\text{C}$. A slope change at 100 °C indicates at least two different mechanisms involved in the conductivity. They may result from conducting Li^+ ions interacting with lattice phonons, or impurities, or structural imperfections. It is also observed from Fig. 1 that σ increases as Ta_2O_5 content increases in the sample. However, the increase of σ is more significant when the doping concentration of Ta_2O_5 is less than 2 mol%. This results from the replacement of La_2O_3 by Ta_2O_5, i.e, large La^{3+} ions (ionic radius 1.2 Å) were replaced by smaller Ta^{5+} ions with 0.7 Å ionic radius. Consequently, La^{3+} ions cannot be located in the glass network but are situated in the openings of the network which prevents the conducting ions, Li^+, from moving in the glass. Therefore, once Ta_2O_5 replaces La_2O_3 in the sample the mobility of Li^+ (originally affected by La^{3+} ions) is increased.

In addition to the replacement of La^{3+} ions by Ta^{5+}, there are two other major effects caused by the Ta_2O_5 doping. These are the opening in the network and the electric field induced by Ta^{5+} ions. At low Ta_2O_5 content i.e., less than 2%, the opening in the network caused by the insert ion of Ta_2O_5, which forms $[TaO_6]$ octahedrons [4], is dominant such that the mobility of Li^+ ions increases and the σ increases accordingly. However, once the doping level of Ta_2O_5 is higher than 2%, the electric field induced by Ta^{5+} ions acting on the Li^+ ions becomes important; hence the rate increase of the Li^+ mobility is diminished. This is why σ increases more slowly when the Ta_2O_5 content is higher than 2% in the sample. Apparently, the electric field is a dominant factor in a 4% Ta_2O_5 sample when the temperature is lower than 100 °C.

3.2. Ta ion implantation

The volume conductivities, σ, of $27Li_2O\text{-}7La_2O_3\text{-}66SiO_2$ sample No. 5, implanted with various fluences of Ta ions, as functions of sample temperatures, T, are shown in Fig. 2. It was observed that σ increases as the fluence of Ta ions increased. This trend is much clearer

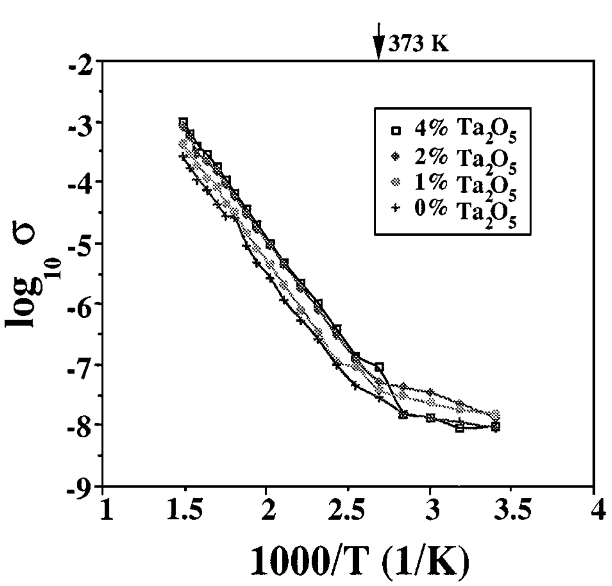

Figure 1 The logarithm conductivities of samples (1–4) as functions of the doping concentrations of Ta_2O_5 at various temperatures.

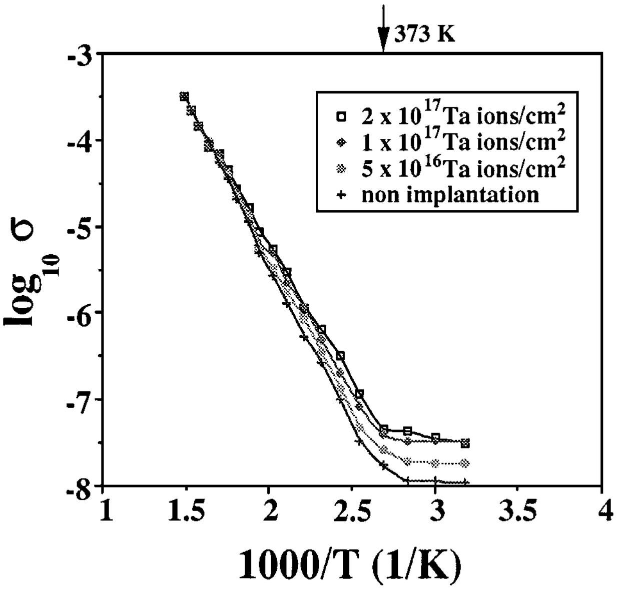

Figure 2 The conductivities of samples as functions of Ta ions fluences in non-Ta_2O_5 sample No. 5 at different temperatures.

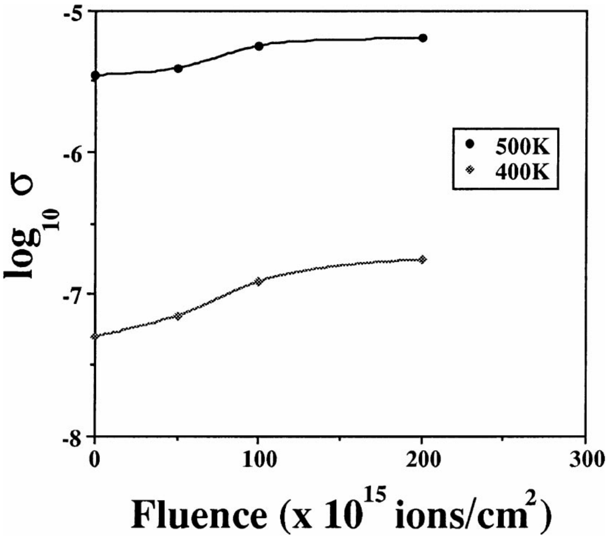

Figure 3 The relationship between Ta^+ ion fluences and logarithms of conductivities in sample No. 5 at 400 and 500 K.

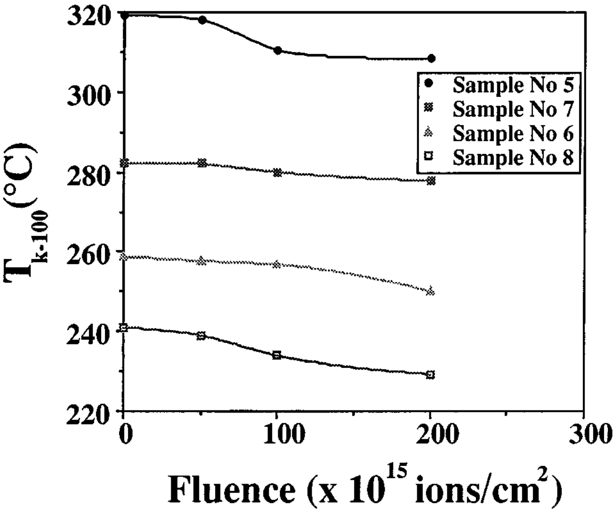

Figure 5 The values of $T_{k\text{-}100}$ of samples as functions of the Ta ion fluences.

when sample temperature is below 270°C. It is obvious that annealing effects take place when the temperature is above 270°C.

Fig. 3 shows the relationship between σ and temperature after sample No. 5 was implanted with various fluences. It is seen that σ increases when annealing temperature and fluence increase.

In order to understand the role of Ta_2O_5 on the conductivity, Ta^+ ions were implanted into both Ta_2O_5 containing sample No. 6 ($27Li_2O$-$7La_2O_3$-$2Ta_2O_5$-64 SiO_2) and non-Ta_2O_5 sample No. 5 samples. The activation energies of conductivity which were deduced from the relation between log σ and $1/T$ in both implanted samples as functions of implantation fluences are plotted in Fig. 4. Activation energies decrease in both samples as the implantation fluence increases. A lower activation energy was also found in the Ta_2O_5 containing sample, which is consistent with the results obtained after Ta_2O_5 doping into the sample.

$T_{k\text{-}100}$ was also determined as a function of Ta fluence in samples No. 5–8 as shown in Fig. 5 where $T_{k\text{-}100}$ is the sample temperature when the conductivity reaches 100×10^{-1} S/cm [5]. It is clearly shown that the higher the Ta fluence in the sample the lower the $T_{k\text{-}100}$. For the samples with the same Li_2O and La_2O_3 contents, i.e., the sample set of No. 5 and 6 and the sample set of No. 7 and 8, it is clearly seen that samples containing less SiO_2 concentration have lower $T_{k\text{-}100}$, i.e., higher conductivity. This results from the presence of less SiO_2 network former which will make Li^+ ions move easier, therefore, the conductivity is higher.

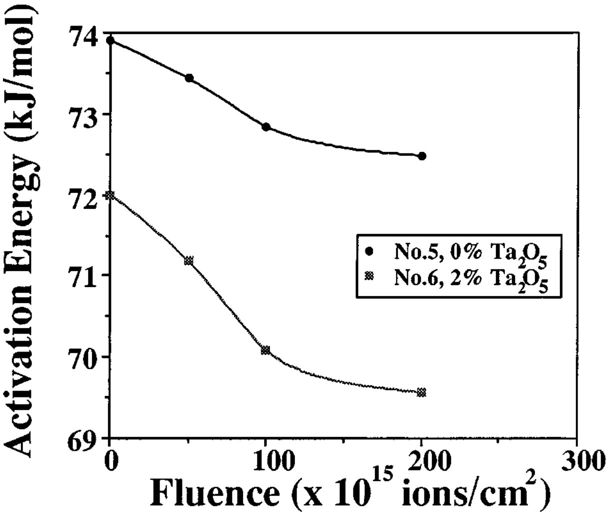

Figure 4 The activation energies of Samples No. 5 and 6 as functions of Ta^+ ion fluences.

Since the changes in conductivity, activation energy and $T_{k\text{-}100}$ of Ta implanted samples are all related to the structural modification induced by the implantation, XPS was used to examine the structure of the samples before and after the implantation. Moreover, it is well known that bridging and nonbridging oxygens (BOs and NBOs) can be used to monitor structural changes in SiO_2 networks [6, 7]. Hence the O 1s photoelectrons were collected and analyzed from samples No. 5 and 6 before and after implantation. The binding energy (BE) of a core level photoelectron of an element was calibrated according to convention by assuming that the binding energy of the surface carbon 1s photoelectron is 284.6 eV [8]. To distinguish non-bridging oxygens from bridging oxygens the decomposition of the asymmetric O 1s peak was carried out, where the bridging oxygen peak was fixed at 532.4 ± 0.1 eV. The binding energy of the non-bridging oxygen component of the O 1s peak was allowed to adjust since the non-bridging oxygen is expected to interact with the implanted Ta cations. Thus the overall best fit for the O 1s peak was obtained. Fig. 6a and b show the decomposed O 1s spectra of sample No. 5 before and after 5×10^{16} Ta^+ ions/cm^2 implantation; NBOs are dramatically increased after implantation.

The results of binding energies, peak areas, and full widths at half maxima of BOs and NBOs before and after implantation are listed in Table II. It is clearly seen that the difference of BEs between BO and NBO is ~1.7 eV before implantation but changes to ~1.4 eV after implantation. This is due to the higher BEs of NBOs after implantation which indicates the

TABLE II The BEs, peak areas, and FWHMs of BOs and NBOs before and after implantation

Sample	Type of Oxygen	BE (eV)	Peak Areas	FWHM (eV)
No. 5, before	BO	532.40	61751	2.31
implantation	NBO	530.63	18026	2.25
No. 5, 5×10^{16}	BO	532.44	42858	2.24
Ta ions/cm^2	NBO	531.00	81322	2.85
No. 5, 1×10^{17}	BO	532.49	21268	1.88
Ta ions/cm^2	NBO	531.07	76757	2.69
No. 6, before	BO	532.40	100667	2.40
implantation	NBO	530.77	44353	2.62
No. 6, 1×10^{17}	BO	532.51	24077	1.96
Ta ions/cm^2	NBO	531.13	78697	2.73

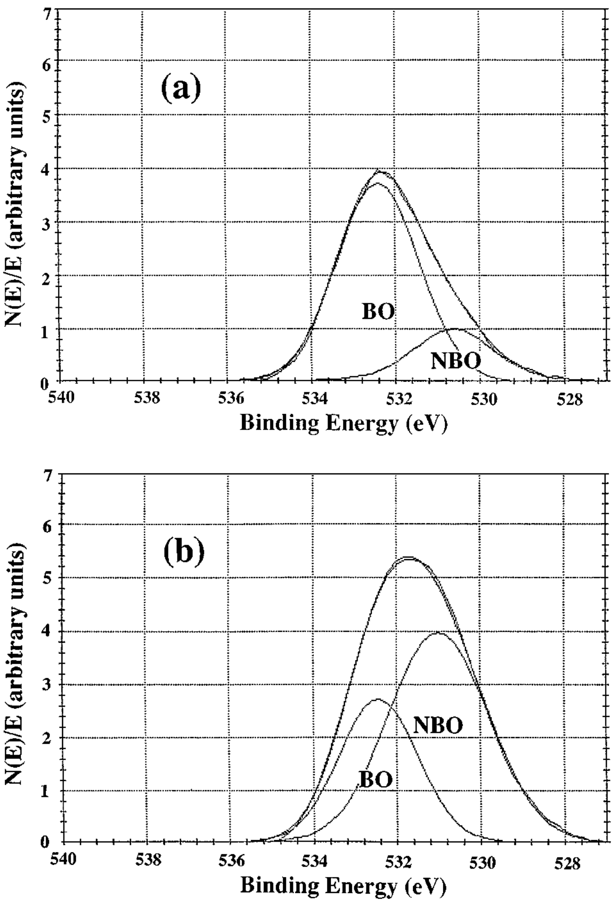

Figure 6 The decomposed O 1s spectra of sample No. 5 (a) before implantation and (b) after 5×10^{16} Ta$^+$ ions/cm^2 implantation. Higher concentration of NBOs was found after the implantation. *It is noted that the overall curve is the whole XPS signal and the two small curves are decomposed BO and NBO peaks.*

electron density around the NBOs shifts towards the Ta cations.

The relative concentrations of BOs and NBOs in the whole O 1s signal are obtained by using the peak areas of BOs and NBOs as shown in Fig. 7. It is noted that more NBOs are found in the Ta_2O_5 containing sample (No. 6) than in the non-Ta_2O_5 sample (No. 5) before implantation. Because the relative concentration of BO decreases and NBO increases in both samples after implantation more openings, conducting channels, are created in the glass such that the conductivity enhances and both activation energy and $T_{k\text{-}100}$ reduce. Consequently, a higher implantation fluence of Ta ions conduct makes Li$^+$ ions much more easily.

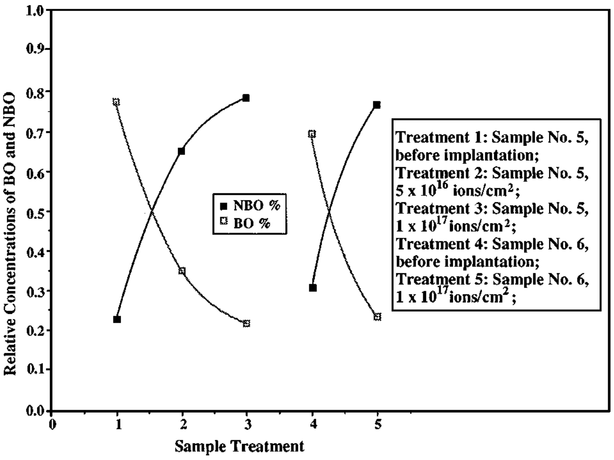

Figure 7 The relative concentrations of BO and NBO in the samples before and after implantation.

4. Conclusions

A linear relationship was found in log σ vs. $1/T$ in Li_2O-La_2O_3-SiO_2 glasses after doping 2 to 4 mol% Ta_2O_5. The higher the doping concentration of Ta_2O_5 the higher the conductivity. It was found in Ta implanted 0% Ta_2O_5 samples that the conductivity is enhanced when the ion fluence is increased, and consequently the activation energies and $T_{k\text{-}100}$ decrease. After being implanted with the same fluence, samples containing Ta_2O_5 show higher conductivity, lower activation energy and lower $T_{k\text{-}100}$ than substrates without Ta_2O_5. Based upon the concentration changes in BOs and NBOs before and after the implantation, more openings or conducting channels are created by implantation in the glass such that the conductivity enhances and both activation energy and $T_{k\text{-}100}$ reduce. It was clearly demonstrated in this study that both doping Ta_2O_5 and implanting Ta ions enhance the conductivity of Li_2O-La_2O_3-SiO_2 electrode glasses.

Acknowledgement

This work was supported in China by the State Key Laboratory for Materials Modification by Laser, Ion and Electron Beams of Dalian University of Technology which is highly appreciated. Work done in the USA was supported by Materials Research Center of Excellence at the University of Texas at El Paso under NSF contract HRD-9353547.

References

1. B. P. NIKOLSKII, A. I. PARFENOV and M. M. SHULTZ, *Doklady Akad. Nauk* **127** (1959) 599. Cited in W. Eitel, "Silicate Science," Vol. 2 (Academic Press, New York, London, 1965) p. 487.
2. A. APPEN, in "Glass Chemistry" (China Architectural Engineering Press, Beijing, 1981) p. 207.
3. J. W. ROSS and M. NEWTON, US Patent no. 394098.
4. M. HUSSAIN, K. NIIHARA and F. FUKUMI, *Mat. Lett.* **24** (1995) 69.

5. G. GEHLHOFF and M. THOMAS, *Z. Tech. Physik* **6** (1925) 544; **7** (1926) 105; **7** (1926) 260.
6. J. S. JEN and M. R. KALINKOWSKI, *J. Non-Crys. Solids* **38/39** (1980) 21.
7. P. W. WANG, L. P. ZHANG, N. BORGEN and K. PANNELL, *J. Mat. Sci.* **31** (1996) 3015.
8. G. M. RENLUND, S. PROCHAZKA and R. H. DOREMUS, *J. Matt. Res.* **6** (1991) 2723.

Received 19 August 1999
and accepted 3 February 2000